

## Vortex dynamics: A variational approach using the principle of least action

Nabil M. Khalifa<sup>\*</sup> and Haithem E. Taha*Mechanical and Aerospace Engineering, University of California, Irvine, California 92697, USA*

(Received 3 August 2023; accepted 13 February 2024; published 22 March 2024)

The study of vortex dynamics using a variational formulation has an extensive history and a rich literature. The standard Hamiltonian function that describes the dynamics of interacting point vortices of constant strength is the Kirchhoff-Routh (KR) function. This function was not obtained from basic definitions of classical mechanics (i.e., in terms of kinetic and potential energies), but it was rather devised to match the already known differential equations of motion for constant-strength point vortices given by the Biot-Savart law. Instead, we develop a variational formulation for vortex dynamics based on the principle of least action. As an application, we consider two-dimensional massive vortices of constant strength. Interestingly, the obtained equations of motion are second-order differential equations defining vortex accelerations, not velocities. The resulting dynamics are more complex than those obtained from the KR formulation. For example, a pair of equal-strength, counter-rotating vortices could be initialized with different velocities, resulting in interesting patterns. Also, the developed model easily admits external body forces. When an electrodynamic force is considered, the interaction between it and the hydrodynamic vortex force leads to a rich, counterintuitive behavior that could not be handled by the KR formulation.

DOI: [10.1103/PhysRevFluids.9.034701](https://doi.org/10.1103/PhysRevFluids.9.034701)

### I. INTRODUCTION

Vortex dynamics represents one of the main pillars of fluid mechanics. The theoretical edifice has been growing since the seminal papers of the founder Helmholtz [1,2]. He introduced the vorticity equations and established the circulation conservation laws when the fluid motion emerges from a potential force. The analogy between potential flow and electricity, discovered by Maxwell [3], has led to simple models of vortex dynamics [4,5]. For example, the standard law that is ubiquitously used in the literature to describe the motion of two-dimensional vortices (infinite vortex filament) is the *Biot-Savart law* [6], which provides first-order ordinary differential equations (ODEs) in the positions of the vortices, in contrast to the second-order ODEs describing any typical dynamics problem. Therefore, it does not permit consideration of arbitrary forces and arbitrary initial velocities of the vortex system.

Kirchhoff and Hensel [7] studied  $N$  free-point vortices of constant strength in an unbounded domain and described their motion based on the Biot-Savart law. Interestingly, the resulting ODEs possessed a Hamiltonian structure [8,9]. Based on this finding, they defined a Hamiltonian function (the Kirchhoff function) for constant-strength point vortices. Interestingly, this Hamiltonian was not derived from basic definitions or first principles. It is not defined in terms of the physical quantities (e.g., kinetic and potential energies) that typically constitute the Hamiltonian function for a mechanical system. It was constructed from the reciprocal property of the stream function of point vortices. Therefore, its use outside this case is questionable and its extension to other

---

\*nkhalifa@uci.edu

scenarios may not be clear, except for a few cases as described below. To account for the interaction with a body, Lin [10,11] provided the most generic and complete formulation of point vortices interacting with a body in two dimensions. He was able to show the existence of a hybrid function  $W$  composed of Kirchhoff's and Routh's functions, which described the Hamiltonian dynamics of a system of vortices and called it the *Kirchhoff-Routh* (KR) function. Arguably, the  $W$  function could be considered as the underlying foundation of every application and study that includes constant-strength point vortices [12–14]. Nevertheless, in all these representations [7,10,11], the resulting ODEs were first order in the position variables.

In this paper, we rely on the principle of least action and its application to the dynamics of a continuum inviscid fluid by Seliger and Whitham [15]. Exploiting this variational principle, we develop a variational formulation for the dynamics of massive vortices of constant strength that are modeled as circular patches (Rankine vortices) with a negligible core size. This effort is considered as a first-order extension of the common vortex dynamics models using the KR function and Biot-Savart law, which takes into account the inertia inside the vortex core. In contrast to previous efforts, the defined Lagrangian and the dynamical analysis are derived from first principles. Interestingly, the formulation presented here results in a second-order ODE defining vortex accelerations, consequently allowing for richer dynamics if the initial velocity is different from the Biot-Savart induced velocity. Moreover, the resulting dynamics recover the KR ODEs in the limit of a vanishing core size. Also, since the model emerges from a formal dynamical analysis, it could take into account different body forces arising from a potential energy. Such a capability is demonstrated in this study by considering an electromagnetic force acting on charged vortices cores. The resulting interaction between the electrodynamic force and the hydrodynamic vortex force leads to a rich, nonlinear behavior that could not be captured by the standard KR formulation.

### A. Background

The study of point vortices interacting with a body has enjoyed significant interest due to its relevance to many applications, e.g., the unsteady evolution of lift over an airfoil due to the interaction of the *starting vortex* with the body [16,17]. Ramodanov [18] studied the interaction of a point vortex with a cylinder (the Föppl problem), then Borisov and Mamaev [19] inspected the integrability of this problem. Moreover, Borisov *et al.* [20,21,22], and Ramodanov and Sokolov [23] extended this setup to allow for multiple point vortices to interact with a cylinder. In another classic article by Shashikanth *et al.* [24], the authors investigated the Hamiltonian dynamics of a cylinder interacting with a number of point vortices. In all of these efforts, the  $W$  function was considered as the main underlying foundation—the Hamiltonian function for the motion of constant-strength point vortices. If time-varying point vortices are considered instead of constant-strength ones, then the  $W$  function will not be applicable because a point vortex of constant strength moves with the local flow velocity (the Kirchhoff velocity) according to Helmholtz laws of vortex dynamics [1], while a vortex with time-varying strength does not, as is well known in the unsteady aerodynamics literature [16,25–29]. As a remedy, Brown and Michael [30] developed a convection model (a first-order ODE in the vortex position) to describe the motion of time-varying point vortices. An alternative model, named the *impulse matching* model, was proposed by Tchieu and Leonard [16] and Wang and Eldredge [26]. Nevertheless, the resulting ODEs from Brown and Michael [30], Tchieu and Leonard [16], and Wang and Eldredge [26] do not have a Hamiltonian structure; they cannot be described by the KR function. An intuitive reasoning for the failure of the KR function in predicting the motion of unsteady point vortices is that, formally, it does not contain any information beyond the Biot-Savart law, and when considered as a Hamiltonian, it is not derived from basic definitions. This argument reveals one of the needs for a variational dynamical framework that is constructed from first principles and capable of describing vortex dynamics, which is the main goal of this article.

While there have been numerous efforts on the Hamiltonian formulation of point vortices, little has been done to develop a Lagrangian framework. This fact may be intuitive given the lack

of veritable dynamics in these Hamiltonian formulations. A true mechanical system will possess both Lagrangian and Hamiltonian formulations, mutually related through the Legendre transformation [8]. However, having an arbitrary Hamiltonian function that happens to reproduce a given set of ODEs does not necessarily represent a mechanical system. As Salmon [31] put it, “*the existence of a Hamiltonian structure is, by itself, meaningless because any set of evolution equations can be written in canonical form.*” These nonstandard Hamiltonians may not be associated with Lagrangian functions. However, there are a few exceptions. For example, Chapman [32] devised a Lagrangian function that reproduces the set of ODEs dictated by the KR Hamiltonian. However, this Lagrangian was not derived from basic definitions or first principles in mechanics (i.e., it is not defined based on the kinetic and potential energies of the system), so it had to be in a nonstandard form (e.g., bilinear in velocity, not quadratic) to result in first-order ODEs, in contrast to the second-order ODEs that typically result from a standard Lagrangian. In a similar spirit, Hussein *et al.* [29] introduced a Lagrangian that reproduces the first-order ODEs of the Brown and Michael [30] model, describing the motion of point vortices with time-varying strength. They used it to study the motion of the starting vortex behind an airfoil and its effect on the lift evolution similar to Wang and Eldredge [26] and Tchieu and Leonard [16].

In contrast to the previously mentioned efforts, there are a few studies that represented a mechanical structure (i.e., second-order ODEs in position) for the vortex motion. Ragazzo *et al.* [33] considered point vortices with finite masses (i.e., massive-point vortices). Using an analogy with electromagnetism, they constructed a Hamiltonian of the massive-point vortices based on that of point charges in a magnetic field. Interestingly, the nonzero inertia of the point vortices (similar to the nonzero charge) resulted in second-order ODEs in position, leading to a richer behavior than that obtained using the KR function. However, the fact that the authors completely relied on the analogy between hydrodynamics and electrodynamics to develop their dynamical model perhaps sets no greater advantage over the devised KR Hamiltonian as far as first principles are concerned. Interestingly, Olva [34] was able to show that their resulting ODEs reduce to those described by the KR function in the limit to a vanishing vortex mass, which, in turn, shows that the KR first-order ODEs is a singularly perturbed representation of Ragazzo *et al.* [33] second-order dynamics. More recently, Richaud *et al.* [35] also considered massive-point vortices, but in a superfluid medium (i.e., Bose-Einstein condensate) using direct numerical simulation of the Gross-Pitaevskii (GP) equation. In addition, they modeled the motion of such vortices using variational principles where the Lagrangian is constructed based on analogy with charged particles subject to magnetic field. They compared the resulting dynamics from both approaches [36,37], which resulted in an almost identical match. Moreover, similar to the results of Ragazzo *et al.* [33], both approaches showed richer dynamics than that obtained by the KR function.

While we did our best to present the relevant literature to the reader, it is certain that we are far from providing a complete account of the perhaps unfathomable literature on the topic. Nor is it our goal here to provide a comprehensive review of such a rich topic. For a thorough review and more information about point-vortex dynamics, the reader is referred to multiple sources [4,5,12–14,25,38–45].

In conclusion, although the previously discussed efforts were quite legitimate and spawned very interesting results [see 14], they suffer from the following drawbacks: (1) the defined Hamiltonian and Lagrangian functions were neither derived from basic definitions in mechanics nor from the available rich literature on variational principles in fluid mechanics [15,31,46–55]; (2) they were either devised to reproduce the already known ODEs or developed based on an analogy with another discipline; (3) as such, the resulting ODEs have no more content beyond the Biot-Savart law; (4) the fact that these functions were not derived from first principles does not allow extension to cases beyond free, constant-strength point vortices. Indeed, one would hope to see a straightforward derivation of the Hamiltonian (or Lagrangian) of point vortices from basic definitions of mechanics (i.e., from kinetic and potential energies) or from the rich legacy of variational principles of continuum fluid mechanics [15,31,46–55], which is the main goal of this work. Such a model

will resolve the drawbacks listed above, resulting in second-order dynamics, allowing extension to unsteady vortices and admitting arbitrary forces (e.g., gravity, electromagnetic, etc).

## II. HAMILTONIAN OF POINT VORTICES: THE KIRCHHOFF-ROUTH FUNCTION

In this section, the KR function for free, constant-strength point vortices in an unbounded flow is presented, demonstrating its Hamiltonian role for constant-strength point vortices. The specified KR function is given by [41]

$$W = \frac{-1}{4\pi} \sum_i \sum_{\substack{j \\ i \neq j}} \Gamma_i \Gamma_j \ln r_{ij}, \quad (1)$$

where  $\Gamma$ 's represent the strengths of the vortices, and  $r_{ij}$  is the relative distance between the  $i$ th and  $j$ th vortices. To show how this function serves as the Hamiltonian of free, constant-strength point vortices, let us recall the stream function describing the flow field at any particular point  $(x, y)$  in the domain

$$\Psi(x, y) = -\frac{1}{2\pi} \sum_i \Gamma_i \ln r_i, \quad (2)$$

where  $r_i$  is the distance between the point  $(x, y)$  and the  $i$ th vortex. As such, the total induced velocity at the  $j$ th vortex (ignoring the vortex self-induction) is given by

$$u_j = \frac{dx_j}{dt} = \frac{-1}{2\pi} \sum_{(i \neq j)} \Gamma_i \frac{(y_j - y_i)}{r_{ij}^2}, \quad v_j = \frac{dy_j}{dt} = \frac{1}{2\pi} \sum_{(i \neq j)} \Gamma_i \frac{(x_j - x_i)}{r_{ij}^2}. \quad (3)$$

Then, multiplying Eq. (3) by  $\Gamma_j$  allows one to write its right-hand side in terms of the scalar function  $W$  as

$$\Gamma_j \frac{dx_j}{dt} = \frac{\partial W}{\partial y_j}, \quad \Gamma_j \frac{dy_j}{dt} = \frac{-\partial W}{\partial x_j}. \quad (4)$$

Defining  $q_j = \sqrt{\Gamma_j} x_j$  and  $p_j = \sqrt{\Gamma_j} y_j$ , it is clearly seen that if  $\Gamma_j$  is constant, then the ODEs (4) are in the Hamiltonian form,

$$\dot{q}_j = \frac{\partial W}{\partial p_j}, \quad \dot{p}_j = \frac{-\partial W}{\partial q_j}, \quad (5)$$

with  $W$  serving as the Hamiltonian.

As demonstrated above, the KR Hamiltonian is not derived from basic definitions of mechanics in terms of kinetic and potential energies. This nonstandard Hamiltonian reproduces the Biot-Savart equations in the Hamiltonian form (5). However, one can relate this function  $W$  to the regularized kinetic energy (KE), as shown in [4,41–43]. The KE ( $T$ ) of the flow field is given by

$$T = -\frac{\rho}{4\pi} \sum_i \sum_{\substack{j \\ i \neq j}} \Gamma_i \Gamma_j \ln r_{ij} - \frac{\rho}{4\pi} \left( \sum_i \Gamma_i^2 \right) \ln \epsilon + \frac{\rho}{4\pi} \left( \sum_i \Gamma_i \right)^2 \ln r_\infty, \quad r_\infty \rightarrow \infty, \epsilon \rightarrow 0, \quad (6)$$

where  $\epsilon$  is a radius of an infinitesimal circle centered at every point vortex and  $r_\infty$  is the radius of the external boundary, which extends to infinity. It is clearly seen that the first term is exactly the  $W$  function scaled by the density  $\rho$  and the last two terms are unbounded as  $r_\infty \rightarrow \infty$  and  $\epsilon \rightarrow 0$ . However, these two unbounded terms are constants and do not depend on the coordinates (i.e., positions of the vortices). As a result, the first term (the *regularized* KE) represents the only variable portion of the infinite KE and was satisfactorily considered as the Hamiltonian of point vortices, while the last two terms are dropped. The previous analysis is notably valid only for constant-strength point vortices and suffers from the several drawbacks discussed in the previous section.

Alternatively, we rigorously develop a model for vortex dynamics from formal variational principles of continuum fluid mechanics, developed by Seliger and Whitham [15].

### III. VARIATIONAL APPROACH AND THE PRINCIPLE OF LEAST ACTION

#### A. The principle of least action

There have been numerous efforts that developed variational principles of Euler's inviscid dynamics [15,31,46–55]. The reader is referred to the thorough review articles of Salmon [31] and Morrison [54]. Also, there have been many efforts that aimed at extending these variational formulations to account for dissipative and/or viscous forces [56–62]. In the current study, we mainly rely on the variational formulation of Euler's equation developed by Seliger and Whitham [15] using the principle of least action.

The principle of least action is typically stated as [8] “*The motion of the system from time  $t_1$  to time  $t_2$  is such that the action integral  $J$  is stationary,*”

$$J = \int_{t_1}^{t_2} \mathcal{L}(q_i, \dot{q}_i, t) dt, \quad (7)$$

where  $\mathcal{L}$  is the Lagrangian function, defined as  $\mathcal{L} = T - V$  where  $T$  and  $V$  are the kinetic and potential energies, respectively, and  $q_i$ 's are the system generalized coordinates. A necessary condition for the functional  $J$  to be stationary is that its first variation must vanish:  $\delta J = 0$ , which, after applying calculus of variation techniques [63], results in the well-known Euler-Lagrange equation

$$\frac{d}{dt} \left( \frac{\partial \mathcal{L}}{\partial \dot{q}_i} \right) - \frac{\partial \mathcal{L}}{\partial q_i} = 0, \quad i = 1, 2, \dots, n. \quad (8)$$

Noticeably, the representation in Eq. (8) describes the dynamics of discrete particles only. However, if a continuum of particles is considered instead, the action integral  $J$  is written in terms of a *Lagrangian density*  $\mathcal{L}_d$  as

$$J = \int_{t_1}^{t_2} \int_{\Omega} \mathcal{L}_d(\mathbf{q}, \dot{\mathbf{q}}, \mathbf{q}_x, \mathbf{x}, t) d\Omega dt, \quad (9)$$

where  $\mathbf{x}$  are the spatial coordinate variables and  $\Omega$  is the spatial domain. In this case, the generalized coordinates  $\mathbf{q}$  are field variables [i.e.,  $\mathbf{q} = \mathbf{q}(\mathbf{x}, t)$ ] and Eq. (8) should be generalized to the continuous system representation [8].

#### B. Variational formulation of Euler's inviscid dynamics: The Lagrangian density is the pressure

The straightforward definition of the action integral for a fluid continuum is

$$J = \int_{t_1}^{t_2} \int_{\Omega} \left[ \frac{1}{2} \rho \mathbf{u}^2 - \rho E(\rho, S) \right] d\Omega dt, \quad (10)$$

where the first term in the integrand represents the KE,  $E$  is the internal energy per unit mass, which represents the potential energy of the fluid continuum, and  $S$  is the entropy whose changes are related to those of  $E$  as

$$dE = \Theta dS - p d(1/\rho), \quad (11)$$

where  $p$  is the pressure and  $\Theta$  is the temperature. Starting with the action (10), through a long and rigorous proof that makes use of Clebsch representation and Lin's constraints, Seliger and Whitham [15] managed to show that the functional  $J$  can be written in the Eulerian formulation as

$$J = - \int_{t_1}^{t_2} \int_{\Omega} p d\Omega dt. \quad (12)$$

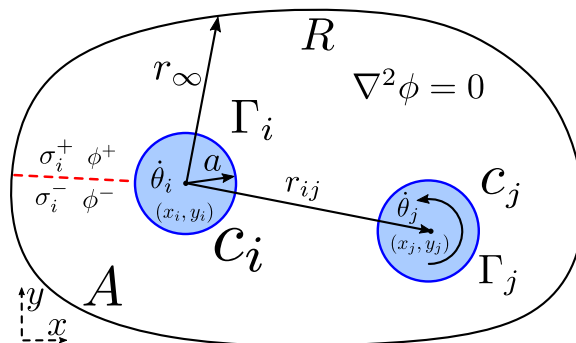


FIG. 1. Schematic drawing for the problem formulation;  $c_i$  is the boundary of the  $i$ th vortex in solid blue,  $\sigma_i$  is the corresponding branch cut (barrier) in dashed red, and  $R$  is the boundary of flow domain in black.

That is, the vanishing of the first variation of  $J$  yields the conservation equations of an inviscid fluid,

$$\frac{\partial \rho}{\partial t} + \nabla \cdot (\rho \mathbf{u}) = 0, \quad (13a)$$

$$\rho \frac{D\mathbf{u}}{Dt} = -\nabla p, \quad (13b)$$

$$\frac{DS}{Dt} = 0. \quad (13c)$$

Hence, Eq. (12) implies that *the Lagrangian density of a continuum of inviscid fluid is the pressure*.

Since the flow outside vortex patches is irrotational by definition, one can use the unsteady Bernoulli equation to write the pressure in terms of the velocity potential  $\phi$ . As such, the principle of least action will then imply that the first variation of the functional,

$$J = \int_{t_1}^{t_2} \int_{\Omega} \rho \left\{ \partial_t \phi + \frac{1}{2} (\nabla \phi)^2 \right\} d\Omega dt, \quad (14)$$

must vanish [15]. This statement is the cornerstone in our analysis for vortex dynamics.

#### IV. VARIATIONAL DYNAMICS OF MASSIVE VORTICES

We apply the proposed variational formulation to develop a model for the dynamics of massive vortices with small core sizes. In particular, we consider  $N$  Rankine vortices; a Rankine vortex is a vortex patch in the two-dimensional plane with a nonzero core size which has a circular boundary; and the fluid inside the core undergoes a rigid-body rotation (i.e., it has constant vorticity over the core). As such, the vortex possesses a nonzero mass (i.e., a massive vortex), in contrast to point vortices which have no mass. The induced flow field outside the vortex core is irrotational [42]. In our formulation, each vortex must have a core (of radius  $a_i$ ) to ensure a finite KE and allow the vortex inertial effects to appear. It is important to mention that constant strengths and radii sizes are considered for simplicity and facilitating comparison with available models in the literature.

The domain consists of an irrotational flow in region  $A$  outside the vortex core and fluid under rigid-body motion inside the core, as shown in Fig. 1. Knowing the vortex strengths *a priori*, the flow velocity  $\mathbf{u}$  at any point  $(x, y)$  in the domain can be written in terms of the locations  $(x_i, y_i)$  of the vortices and their derivatives,

$$\mathbf{u}(x, y) = \mathbf{u}(x_i, y_i, \dot{x}_i, \dot{y}_i; \Gamma_i). \quad (15)$$

This representation is the foundation of the current analysis; the flow velocity in the entire domain depends only on a finite number of variables  $(x_i, y_i)$ . That is, Eq. (15) represents a model reduction from an infinite number of degrees of freedom down to only  $2N$ . As such, the principle of least

action, and analytical mechanics formulation in general, are especially well suited for this problem because it allows one to accept the given kinematical constraints (15) and focus on the dynamics of the reduced system ( $2N$  degrees of freedom), in contrast to the Newtonian-mechanics formulation where such a reduction is not possible. Rather, the large system must be retained (i.e., a partial differential equation (PDE) for the infinite system at hand) and the kinematic constraint (15) will be associated with an unknown constraint force in the equations of motion of the large system (in the PDE).

The above description implies that the Lagrangian has two contributions,

$$\mathcal{L} = \mathcal{L}_\phi + \mathcal{L}_C, \quad (16)$$

where  $\mathcal{L}_\phi$  is the Lagrangian of the irrotational flow outside the cores and  $\mathcal{L}_C$  is the core Lagrangian. The action integral is then given by

$$J = \int_{t_1}^{t_2} \left( \int_A \mathcal{L}_{d_\phi} dA + \mathcal{L}_C \right) [x_i(t), y_i(t), \dot{x}_i(t), \dot{y}_i(t); \Gamma_i] dt, \quad (17)$$

where  $\mathcal{L}_{d_\phi}$  is the Lagrangian density of the continuum field, which is  $-p$ , as shown by Seliger and Whitham [15] and presented in the previous section. After integrating the fluid Lagrangian density  $\mathcal{L}_{d_\phi}$  over space, the problem could be treated as one with finite degrees of freedom ( $x_i, y_i$ )—akin to particle mechanics.

The Lagrangian of the core flow under rigid-body motion in the horizontal plane (i.e., no active gravitational forces) is

$$\mathcal{L}_C = \sum \frac{m_i}{2} \mathbf{u}_i \cdot \mathbf{u}_i + \sum \frac{I_i}{2} \dot{\theta}_i^2, \quad (18)$$

where  $m_i$  is the fluid mass inside the  $i$ th vortex core and  $I_i$  is its moment of inertia. As mentioned before, constant-strength vortices are considered. Hence, the angular velocity  $\dot{\theta}_i$  of each rigid core (which is proportional to  $\Gamma_i$ ) is constant. This immediately forces the  $\theta$  coordinate to be an ignorable (i.e., cyclic) coordinate [9]. In other words, the corresponding momentum  $\partial \mathcal{L}_C / \partial \dot{\theta}$  is constant. It now remains to compute the Lagrangian of the continuum fluid outside the cores in terms of the generalized coordinates  $\mathbf{q} = (x_1, y_1, \dots, x_N, y_N)$ .

### A. Irrotational flow Lagrangian computation

The Lagrangian density of the inviscid fluid, as discussed in Sec. III B, is the pressure. It is given by Eq. (14), where the second term is the flow KE and the first term is due to the  $\partial_t \phi$  term.

#### 1. Flow KE

Consider the flow KE of the irrotational flow field in Fig. 1,

$$T = \frac{\rho}{2} \int_A \mathbf{u} \cdot \mathbf{u} dA = \frac{\rho}{2} \int_A (\nabla \phi)^2 dA, \quad (19)$$

where  $A$  is the irrotational flow field domain. After following the analysis in Appendix A, the KE can be written as

$$T = -\frac{\rho}{2} \left[ \sum_{i \neq j} \sum \Gamma_i \psi_j|_i + \sum \Gamma_i \psi_i|_{c_i} + \Psi|_R \Gamma_R + \sum \Gamma_i \Psi|_R \right], \quad (20)$$

where  $\psi_j|_i$  is the stream function of the irrotational flow induced by the  $j$ th vortex evaluated at the center of the  $i$ th one (this is applicable as long as  $r_{ij} \gg a$ ),  $\psi_i|_{c_i}$  is the  $i$ th vortex stream function evaluated over its boundary  $c_i$ ,  $\Psi|_R$  is the total stream function (due to all vortices; i.e.,  $\Psi = \sum_j \psi_j$ ) evaluated at the boundary  $R$ , and  $\Gamma_R$  is the circulation over the same boundary. For an irrotational flow,  $\Gamma_R$  is the sum of all circulations inside the domain (i.e.,  $\Gamma_R = \sum_i \Gamma_i$ ). The fourth term results from the multivalued nature of the potential function  $\phi$  when evaluated over the fictitious barrier  $\sigma_i$

for the  $i$ th vortex. Equation (20) is then written as

$$T = -\frac{\rho}{4\pi} \sum_{i \neq j} \Gamma_i \Gamma_j \ln r_{ij} - \frac{\rho}{4\pi} \left( \sum \Gamma_i^2 \right) \ln a + \frac{\rho}{4\pi} \left( \sum \Gamma_i \right)^2 \ln r_\infty - \frac{\rho}{2} \Psi|_R \Gamma_R, \quad (21)$$

where  $a$  is the core radius. The terms in Eq. (20) can be compared to the regularized KE presented in Eq. (6). The first term is exactly the KR function for free  $N$  point vortices, while the second terms in both match with the core radius  $a$  taking the place of the limit circle radius  $\epsilon$ . Also, the third terms match, which will blow up for unbounded flows unless the total circulation is zero. The fourth term in Eq. (20) is an additional term that is not captured in Eq. (6). However, similar to the third term, it is infinite for unbounded flows unless  $\Gamma_R = 0$ . In fact, the main reason behind the boundedness of the last two terms in the case of zero total circulation is that the velocity will be of the order of  $\sim \mathcal{O}(1/r^2)$  in contrast to  $\sim \mathcal{O}(1/r)$  for a nonzero total circulation [12].

It is important to mention that if the vortex boundary deforms, it will result in a time-varying moment of inertia  $I(t)$ , precluding the cyclic nature of the angular motion  $\theta$  even for constant-strength vortices. In this study, however, we ignore such changes in the vortex boundary shape. This is a reasonable assumption as long as the distance between the vortices is considerably larger than the vortex core size [4]. In other words, vortex patches could interact and deform when they are close to each other; this behavior is studied as a *contour dynamics* problem [42,64,65], where Melander *et al.* [66] provided a Hamiltonian representation for it. However, in this first-order study, we are concerned with vortex patches concentrated in tiny cores and hence ignore the effect of shape deformation, which is one step beyond the point-vortex model. Luckily, it was shown by Deem and Zabusky [67], Pierrehumbert [68], and Saffman and Szeto [69] that any vortex pairs distantly apart from each other, as long as  $a/b \ll 1$  where  $b$  is half the distance between the two vortices center, will behave as if they were point vortices and not deform the boundary of each other.

## 2. $\partial_t \phi$ contribution to the Lagrangian

The total flow potential function is defined as

$$\phi = \sum_i \phi_i, \quad (22)$$

where  $\phi_i$  is the potential function of the flow associated with the  $i$ th vortex, which depends on  $[x, y, ; x_i(t); y_i(t); \Gamma_i]$ . That is, it does not have an explicit time dependence. Rather, its time derivative will be a convectivelike term with respect to the Lagrangian coordinates  $(x_i, y_i)$ ,

$$\partial_t \phi = \sum_i \mathbf{u}_i \cdot \nabla_i \phi_i. \quad (23)$$

As such, the  $\partial_t \phi$  contribution to the Lagrangian can be written as

$$\mathcal{L}_{\phi_i} = \rho \int_A \partial_t \phi dA = \rho \int_A \sum_i \mathbf{u}_i \cdot \nabla_i \phi_i dA, \quad (24)$$

whose direct computation is cumbersome. Instead, we will apply Eq. (8) first. For example, consider the term  $\partial \mathcal{L}_{\phi_i} / \partial \dot{x}_i$ , which is needed for the  $x_i$  equation of motion. By definition, we have

$$\frac{\partial \mathcal{L}_{\phi_i}}{\partial \dot{x}_i} = \rho \partial_{\dot{x}_i} \int_A \sum_i \mathbf{u}_i \cdot \nabla_i \phi_i dA, \quad (25)$$

where the differentiation can be pushed forward within the integral because the integral bounds are independent of the vortex velocity  $\dot{x}_i$ . As such, all terms will vanish except

$$\frac{\partial \mathcal{L}_{\phi_i}}{\partial \dot{x}_i} = \rho \int_A \partial_{\dot{x}_i} \phi_i dA. \quad (26)$$

Moreover, since there is no explicit time dependence and assuming constant-strength vortices, the time derivative of Eq. (26) is

$$\frac{d}{dt} \left( \frac{\partial \mathcal{L}_{\phi_t}}{\partial \dot{x}_i} \right) = \rho \mathbf{u}_i \cdot \nabla_i \left( \int_A \partial_{x_i} \phi_i dA \right) = \rho \left\{ \dot{x}_i \partial_{x_i} \int_A \partial_{x_i} \phi_i dA + \dot{y}_i \partial_{y_i} \int_A \partial_{x_i} \phi_i dA \right\}. \quad (27)$$

Similarly, the other derivative  $\partial \mathcal{L}_{\phi_t} / \partial x_i$  needed for the  $x_i$  equation is written as

$$\frac{\partial \mathcal{L}_{\phi_t}}{\partial x_i} = \rho \partial_{x_i} \int \sum_j \mathbf{u}_j \cdot \nabla_j \phi_j dA = \rho \left\{ \dot{x}_i \partial_{x_i} \int_A \partial_{x_i} \phi_i dA + \dot{y}_i \partial_{x_i} \int_A \partial_{y_i} \phi_i dA \right\}. \quad (28)$$

Consequently, subtracting Eq. (28) from Eq. (27) will result in the cancellation of the first term in the  $x_i$  equation of motion. As such, we have

$$\frac{d}{dt} \left( \frac{\partial \mathcal{L}_{\phi_t}}{\partial \dot{x}_i} \right) - \frac{\partial \mathcal{L}_{\phi_t}}{\partial x_i} = \rho \dot{y}_i \left[ \partial_{y_i} \int_A \partial_{x_i} \phi_i dA - \partial_{x_i} \int_A \partial_{y_i} \phi_i dA \right], \quad (29)$$

which, after the detailed computation presented in Appendix B, yields

$$\frac{d}{dt} \left( \frac{\partial \mathcal{L}_{\phi_t}}{\partial \dot{x}_i} \right) - \frac{\partial \mathcal{L}_{\phi_t}}{\partial x_i} = \rho \dot{y}_i \left[ \sum_{\substack{j \\ i \neq j}} \left( \int_{c_j} \partial_{x_i} \phi_i dx - \int_{c_j} \partial_{y_i} \phi_i dy \right) - \Gamma_i \right], \quad (30)$$

where the final integrals are evaluated numerically over the  $j$ th vortex boundary  $c_j$ . Also, for clarity and brevity, the numerical integrals are denoted as

$$I_{x_{ij}} = \int_{c_j} \partial_{x_i} \phi_i dx, \quad I_{y_{ij}} = \int_{c_j} \partial_{y_i} \phi_i dy, \quad (31)$$

resulting in the final form

$$\frac{d}{dt} \left( \frac{\partial \mathcal{L}_{\phi_t}}{\partial \dot{x}_i} \right) - \frac{\partial \mathcal{L}_{\phi_t}}{\partial x_i} = \rho \dot{y}_i \left[ \sum_{\substack{j \\ i \neq j}} (I_{x_{ij}} - I_{y_{ij}}) - \Gamma_i \right]. \quad (32)$$

Similarly, the  $y_i$  equation is

$$\frac{d}{dt} \left( \frac{\partial \mathcal{L}_{\phi_t}}{\partial \dot{y}_i} \right) - \frac{\partial \mathcal{L}_{\phi_t}}{\partial y_i} = \rho \dot{x}_i \left[ \sum_{\substack{j \\ i \neq j}} (I_{y_{ij}} - I_{x_{ij}}) + \Gamma_i \right]. \quad (33)$$

## B. Equations of motion

We are now ready to write the final form of the equations of motion from the Euler-Lagrange equation (8), where  $\mathbf{q} = (x_1, y_1, \dots, x_N, y_N)$ , the Lagrangian  $\mathcal{L} = \mathcal{L}_\phi + \mathcal{L}_C$ , and the contributions of different terms are given in Eqs. (21), (18), (32), and (33).

Substituting Eqs. (21), (18), (32), and (33) into the Euler-Lagrange equation (8), while assuming the motion taking place in a horizontal plan, we obtain

$$m_i \ddot{x}_i + \frac{\rho \Gamma_i}{2\pi} \sum_j \Gamma_j \frac{(x_i - x_j)}{r_{ij}^2} + \rho \dot{y}_i \left[ \sum_{\substack{j \\ i \neq j}} (I_{x_{ij}} - I_{y_{ij}}) - \Gamma_i \right] = 0, \quad (34)$$

$$m_i \ddot{y}_i + \frac{\rho \Gamma_i}{2\pi} \sum_j \Gamma_j \frac{(y_i - y_j)}{r_{ij}^2} + \rho \dot{x}_i \left[ \sum_j (I_{y_{ij}} - I_{x_{ij}}) + \Gamma_i \right] = 0, \quad (35)$$

with noting  $m_i = \rho \pi a^2$ , which results in

$$\ddot{x}_i = -\frac{\Gamma_i}{2\pi^2 a^2} \sum_j \Gamma_j \frac{(x_i - x_j)}{r_{ij}^2} - \frac{\dot{y}_i}{\pi a^2} \left[ \sum_j (I_{x_{ij}} - I_{y_{ij}}) - \Gamma_i \right], \quad (36)$$

$$\ddot{y}_i = -\frac{\Gamma_i}{2\pi^2 a^2} \sum_j \Gamma_j \frac{(y_i - y_j)}{r_{ij}^2} - \frac{\dot{x}_i}{\pi a^2} \left[ \sum_j (I_{y_{ij}} - I_{x_{ij}}) + \Gamma_i \right]. \quad (37)$$

These equations represent the sought dynamical equations that describe the dynamics of free massive vortices from first principles: the principle of least action. They are second order in nature and capture inertial effects of the core. In particular, they allow enforcing an initial condition on velocity, similar to any typical problem in dynamics. Moreover, the analysis allows for extension to time-varying vortices where  $\dot{\Gamma}$  terms appear. Also, arbitrary conservative forces (e.g., gravitational, electric) can be incorporated in this framework, in contrast to the standard analysis based on the KR function. Interestingly, in the limit of a vanishing core size ( $a \rightarrow 0$ ),  $m_i$ ,  $I_{x_{ij}}$ , and  $I_{y_{ij}}$  go to zero and the resulting dynamics (36) and (37) reduce to the first-order equations given by the KR Hamiltonian. However, for finite-size cores, the new dynamics given by Eqs. (36) and (37) are richer than the first-order equations of the KR Hamiltonian, which recover the Biot-Savart law. To show the value of the proposed formulation, some case studies are presented below.

## V. CASE STUDIES

Different case studies are presented to highlight the similarity and differences between the motions resulting from the proposed model and the standard KR model (i.e., Biot-Savart law). As pointed out above, the proposed variational dynamics result in the KR solution for small vortex radii. One of the major differences between the two formulations is that the KR equations are first order, allowing only initial conditions of vortex position to be assigned, whereas the proposed equations are second order, admitting arbitrary initial velocities in addition. Therefore, the similarity between the resulting two motions does not necessarily happen when the initial velocities do not match the induced velocities by the Biot-Savart law.

### A. Vortex pairs initialized with arbitrary velocities

Equal strength vortex pairs are considered in Fig. 2 with radius  $a = 1$  and  $\Gamma = 10\pi$ . The trajectories of the vortex pairs are presented in comparison to the KR motion. The trajectory of a counter-rotating vortex pair is shown in Fig. 2(a), while Fig. 2(b) shows the trajectory of a co-rotating pair. For this case of small vortex cores (in comparison to the relative distance), when the model is initialized with the Biot-Savart induced velocity, almost-exact matching with the KR motion (black trajectory in Fig. 2) is obtained. However, when the proposed model is initialized with a different value in the same direction, the resulting dynamics (red and blue trajectories in Fig. 2) are richer. The resulting motion is composed of fast and slow timescales. The slow dynamics (average solution) possesses a similar behavior to the KR one (in many but not all cases, as shown below); around this averaged response, there are oscillations in the fast timescale.

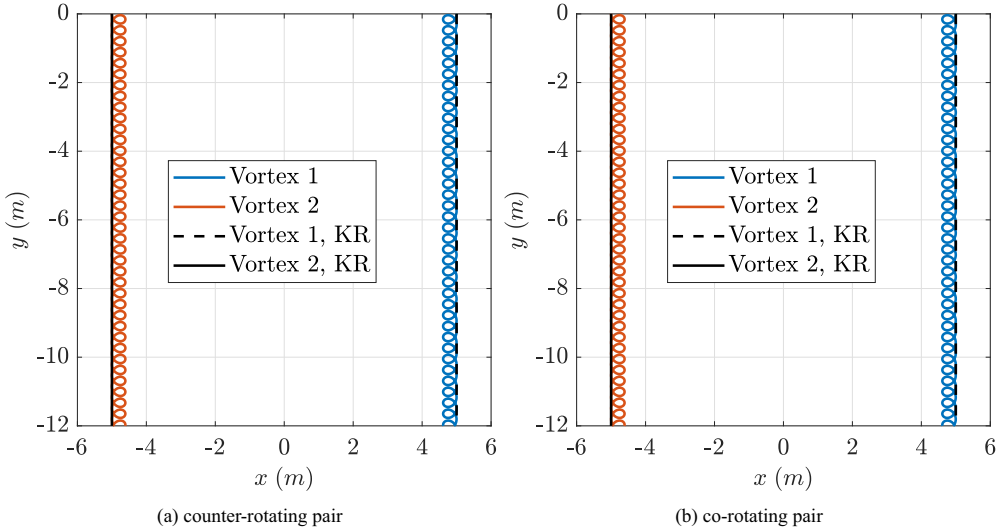


FIG. 2. Simulation of proposed variational vortex dynamics model against the KR model for a pair of vortices. The initial velocities are set to five multiples of the Biot-Savart induced velocity in the same direction.

The behavior of the slow dynamics is not always similar to that of the KR model. In Fig. 3, a pair of counter-rotating vortices is simulated and the system is initialized with the Biot-Savart induced velocity (i.e., down); however, the vortex on the right is given an additional initial velocity to the right. These initial conditions resulted in quite different averaged behaviors of the two vortices, as shown in Fig. 3. The effect of the initial velocity on the averaged motion of interacting vortices, as demonstrated above, points to some interesting applications of vortex motion control. Imagine a large vortex which we are interested in deviating its motion from an anticipated trajectory. One can then pose the interesting question: Can we set a group of vortices in motion with specified initial velocities in the neighborhood of the large vortex so that its net motion deviates from the anticipated

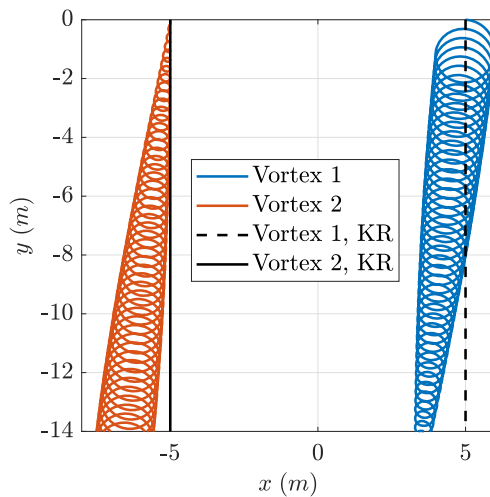


FIG. 3. Simulation of the variational vortex dynamics model presenting the deviation of a counter-rotating vortex pair from the KR trajectory. Initial velocities for the vortices are  $u_{10} = (10i, -0.5j)$  and  $u_{20} = (0i, -0.5j)$ , respectively.

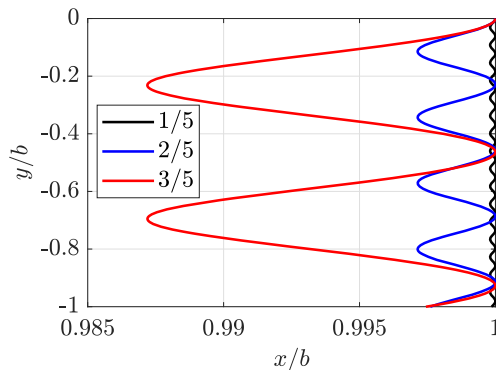


FIG. 4. Sensitivity study for different  $a/b$  ratios. Trajectories for the right-hand side vortex are presented. The scale is adjusted to emphasize the differences between each of the cases.

trajectory in the absence of these vortices? Using a similar approach to the one presented above, one can answer such a question.

A sensitivity study is carried out in an attempt to quantify the fast oscillation dynamics that is superimposed over the regular KR solution. The amplitude and frequency of oscillation are characterized against different  $a/b$  ratios. This study is performed on the example of a counter-rotating pair initialized with the Biot-Savart induced velocity. The resulting trajectories of the right-hand-side vortex, scaled with respect to the half-separating distance  $b$ , are shown in Fig. 4. The plots demonstrate the oscillation dynamics for different values of  $a/b$ . It is evident that the amplitude of oscillation is directly proportional to  $a/b$ ; however, the oscillation frequency is inversely proportional to this ratio. A qualitative description of the underlying phenomenon could be deduced from the (introduced) acceleration terms, which account for inertial effects in the equations of motion by considering the vortex mass. Hence, larger vortices tend to oscillate slower with large amplitudes, and vice versa. It is not easy to quantify these effects analytically due to the strong nonlinearities in the equations of motion. However, approximate analytical expressions could be obtained using perturbation techniques (e.g., the method of multiple scales [70,71]).

### B. Hydrodynamic and electrodynamic forces interaction

To further demonstrate the capability of the developed vortex model to capture dynamical features that cannot be directly captured by the usual KR formulation, we consider a charged particle inside the core of each vortex and that the motion takes place in the presence of a constant-strength electric field. In this case, each vortex will experience a *Lorentz* force  $\mathbf{F} = q\mathbf{E}$ , where  $q$  is the particle's charge and  $\mathbf{E}$  is the electric field vector. The effect of this electric field on the motion of the vortex system cannot be directly obtained from the standard formulation using the KR function. A true dynamical formulation is invoked instead. It is straightforward to account for this effect using the developed dynamical formulation where forces can be considered. Simply, the right-hand sides of Eqs. (36) and (37) will be modified by adding  $q_i E_x/m_i$  and  $q_i E_y/m_i$ , respectively, where  $E_x$  and  $E_y$  are the components of the electric field in the  $x$  and  $y$  directions, respectively, and  $q_i$  is the charge of the  $i$ th vortex. Alternatively, one can add  $-\sum_i q_i \Phi(x_i, y_i)$  to the Lagrangian function, where  $\Phi$  is the scalar electrostatic potential ( $\mathbf{E} = -\nabla\Phi$ ). For simplicity, we considered a large electric field and small charges so that the *Coulomb* force is negligible with respect to the Lorentz force. In the following simulations, we considered  $|q\mathbf{E}|/m = g$ , where  $g$  is the gravitational acceleration, and all motions are initialized with the KR velocities.

Figure 5 shows a pair of counter-rotating vortices of the same strength and the same charge placed in an electric field of constant strength. Figure 5(a) shows the resulting motion when the electric field is pointing downward (negative  $y$ ). This implies that the vortices will accelerate downward beyond

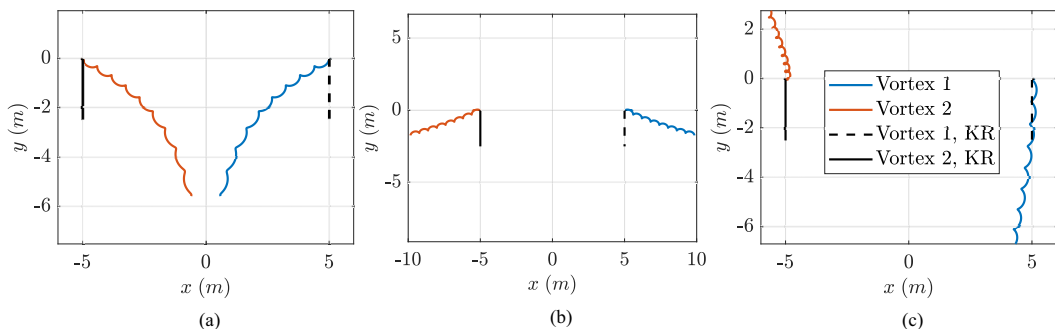


FIG. 5. Different simulations for counter-rotating pair of vortices with same charge placed in a constant-strength electric field. Simulations are initialized by the Biot-Savart induced velocity and electric field direction for each case is listed as (a)  $\mathbf{E} \downarrow$ , (b)  $\mathbf{E} \uparrow$ , and (c)  $\mathbf{E} \rightarrow$ .

the KR value dictated by the Biot-Savart law, which will in turn cause an acceleration in the  $x$  direction because of the term  $\dot{y}_i \Gamma_i$  in Eq. (36). As a result, the two counter-rotating vortices attract towards one other. Note that the simulation should not be deemed valid when the vortices get very close to each other. On the other hand, reversing the direction of the electric field (i.e., opposite to the KR velocity), the KR  $y$  motion is decelerated, leading the counter-rotating vortices to repel, as shown in Fig. 5(b). Interestingly, applying an electric field in the horizontal direction ( $+x$ ), we obtain the response in Fig. 5(c), which is nonintuitive. Although the applied electric force is in the  $x$  direction, the net effect is much more significant in the  $y$  direction. Moreover, even the effect in the  $x$  motion is counterintuitive; both vortices drift in the negative  $x$  axis (opposite to the direction of the applied electric force). At the beginning, there is an acceleration for both vortices in the  $x$  direction. However, the slightest velocity in  $x$  activates the term  $-\dot{x}_i \Gamma_i$  in the  $\ddot{y}_i$  in Eq. (37), which causes a downward acceleration for the right vortex and an upward acceleration for the left vortex (of negative strength). These vertical accelerations, in turn, affect the  $x$  motion through the term  $\dot{y}_i \Gamma_i$  in Eq. (36), causing both vortices to drift to the left (opposite to the applied force). This interesting interaction between the motion induced by the electric force and the motion induced by the *vortex force* ( $\dot{y}_i \Gamma_i, -\dot{x}_i \Gamma_i$ ) is naturally captured in the developed dynamic model. Although the KR motion is not really relevant here, it is presented for comparison in Figs. 5 and 6.

Figure 6 shows the motion of a pair of counter-rotating vortices of equal strength, but of equal and opposite charges placed in a constant-strength electric field. Figure 6(a) shows the response

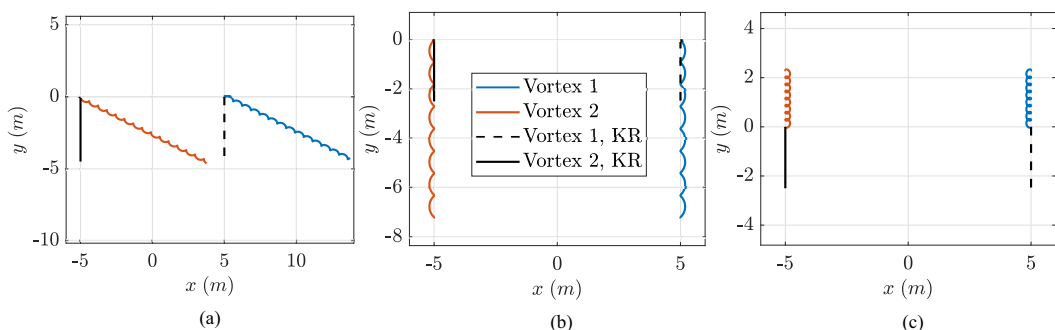


FIG. 6. Different simulations for counter-rotating pair of vortices with opposite charge placed in a constant-strength electric field. Simulations are initialized by the Biot-Savart induced velocity; electric field direction and charge sign for each case are listed as (a)  $\mathbf{E} \uparrow$ ,  $+q_1$ , and  $-q_2$ , (b)  $\mathbf{E} \rightarrow$ ,  $+q_1$ , and  $-q_2$ , and (c)  $\mathbf{E} \rightarrow$ ,  $-q_1$ , and  $+q_2$ .

to an upward electric field causing an upward force on the right vortex (with positive charge) and a downward force on the left vortex (with negative charge). Yet, both vortices move downward and the significant effect is a drift in the  $x$  direction due to the interaction mentioned above: the downward acceleration of the left vortex causes an acceleration in the  $x$  direction through the term  $\dot{y}_i \Gamma_i$  in Eq. (36), which in turn causes an upward acceleration through the term  $-\dot{x}_i \Gamma_i$  in Eq. (37). Similar behavior occurs with the right vortex; initially, it experiences an upward acceleration from the electric force, which causes an  $x$  acceleration through the term  $\dot{y}_i \Gamma_i$  in Eq. (36). This  $x$  motion, in turn, causes a negative  $y$  acceleration through the term  $-\dot{x}_i \Gamma_i$  in Eq. (37). As a result, the right vortex, though forced by an upward force, moves to the right and downward, which is a quite nonintuitive behavior.

Figure 6(b) shows the response to an electric field in the  $x$  direction, causing a right force on the right vortex and a left force on the left vortex (with the opposite charge); i.e., pulling the vortices away from each other. However, no considerable net effect is observed in contrast to the other scenarios. The initial right motion of the right vortex due to the electric force causes a downward acceleration, which in turn causes a negative  $x$  acceleration that opposes the electrodynamic acceleration. The situation leads to an equilibrium with a periodic solution close to the KR motion. The behavior in Fig. 6(c) is quite interesting, which presents the motion due to an electric field to the left, causing a left force on the right vortex and a right force on the left vortex; i.e., pushing the vortices towards one another. However, the response is counterintuitive as usual due to the interesting interaction between the electrodynamic force and the hydrodynamic vortex force. Instead of getting closer to each other (to comply with the applied force), the two vortices move upward opposite to their initial KR velocity. As usual, the vortices initially follow the applied electric force (i.e., get closer to one another). This  $x$  motion causes an upward acceleration to both vortices, which causes an  $x$  acceleration opposite to the electrodynamic one for both vortices.

The interaction between the electrodynamic force and the vortex force ( $\dot{y}_i \Gamma_i$  in the  $x$  direction and  $-\dot{x}_i \Gamma_i$  in the  $y$  direction) leads to very interesting behaviors: when pulling vortices downward (i.e., in the same direction as their KR initial velocity), they attract [Fig. 5(a)]; when pulling them upward (i.e., opposite to their KR initial velocity), they repel [Fig. 5(b)]; when they are pushed together to the right, they both end up moving to the left with one upward and one downward [Fig. 5(c)]; when pulling them away from each other, they almost did not respond [Fig. 6(b)]; and when pushing them towards one another, they move upward [Fig. 6(c)]. It is quite nonintuitive, yet explainable from the physics of the dynamic model in Eqs. (36) and (37). This nonlinear behavior presents the dynamic model [Eqs. (36) and (37)] as a rich mechanical system for geometric mechanics and control analysis using Lie brackets [72–74] where the concepts of *anholonomy* [75], geometric phases [76,77], and nonlinear controllability [78,79] can be demonstrated.

## VI. VALIDATION

In this section, the resulting dynamics from the proposed variational formulation is validated against the available data from the literature, particularly the results of Ragazzo *et al.* [33] and Richaud *et al.* [36,37]. The current validation is established on the fact that the results of Richaud *et al.* [36,37] using the Hamiltonian proposed by Ragazzo *et al.* [33] were validated against direct numerical simulation of the GP equation for a superfluid (i.e., an inviscid fluid). Hence, the results of Ragazzo *et al.* [33] are deemed credible according to the validation against direct numerical simulations of GP. Nevertheless, the Hamiltonian adopted by Ragazzo *et al.* [33] and Richaud *et al.* [36,37] was devised based on analogy with electrodynamics and was not formally derived from variational principles of classical fluid mechanics, in contrast to the current effort. As mentioned before, the proposed variational model recovers the KR dynamics for coreless and massless vortices when the vortices are initialized with the Biot-Savart induced velocity. However, as shown in Sec. V, the proposed model introduces intriguing dynamics when initialized with various velocities, and when body forces are included. For instance, if coreless, but massive point vortices are considered (in this case, the integrals  $I_{x_{ij}}$ ,  $I_{y_{ij}}$  vanish, but the core mass  $m_i$  is retained), then the resulting

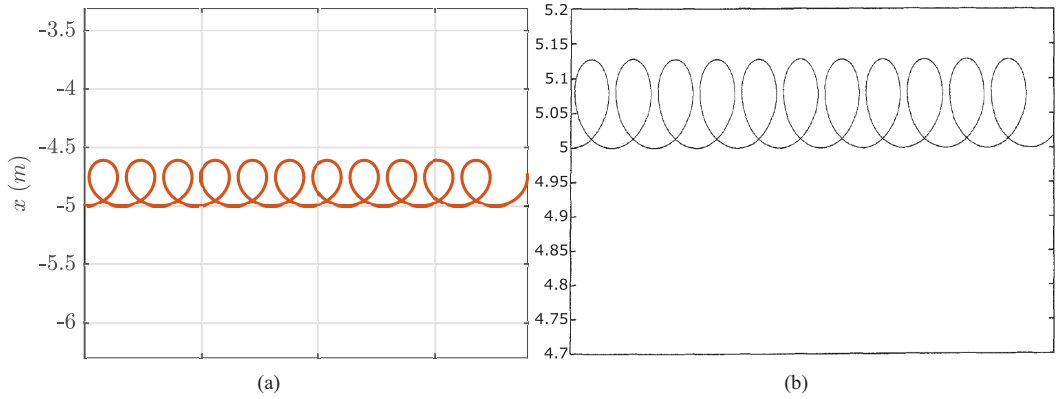


FIG. 7. Comparison between the proposed variational vortex dynamics model and the model of Ragazzo *et al.* [33] when vortices are initialized with a velocity different from the Biot-Savart induced velocity. (a) Simulation of a counter-rotating pair initialized with five multiples of the Biot-Savart induced velocity, showing only one vortex. (b) Counter-rotating pair simulated as a single vortex in the half plane [33].

dynamics could be compared against Ragazzo *et al.* [33]. Interestingly, the resulting equations of motion along with the Hamiltonian (see Appendix C) from the proposed variational model reduce to those deduced by Ragazzo *et al.* [33]. The similarity between the equations of motion and the Hamiltonian between the two approaches is reinforced by the matched trajectories, as shown in Fig. 7. Moreover, the resulting dynamics are compared against Richaud *et al.* [36] in Figs. 8 and 9, highlighting almost exact matching. The recovery of the proposed formulation to the special cases of the KR formulation, Ragazzo's and Richaud's formulation provides credibility to the presented approach.

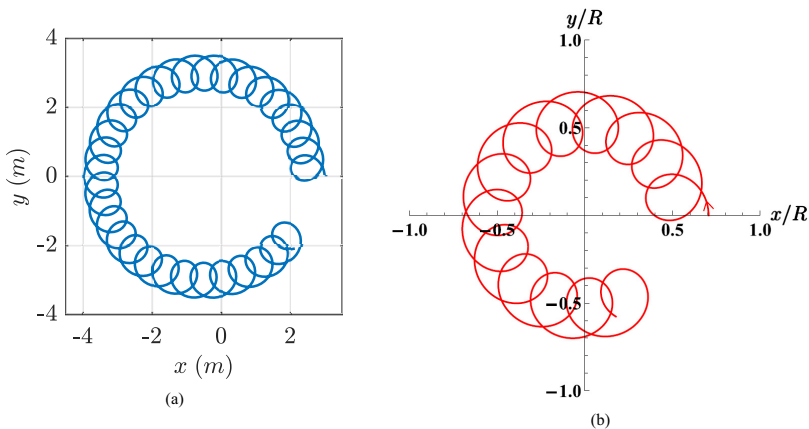


FIG. 8. Comparison between the proposed variational vortex dynamics model and Richaud *et al.* [36] model. Vortices are initialized with a velocity different from the Biot-Savart induced velocity. (a) Simulation of co-rotating pair initialized with  $u_{1_0} = (0i, 5.83j)$  and  $u_{2_0} = (0i, 4.16j)$ , showing only the first vortex on the right-hand side. (b) Single vortex simulated in a confined circular domain [36].

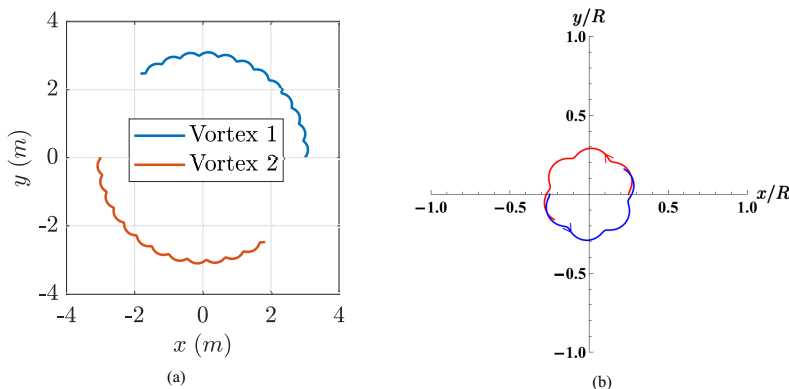


FIG. 9. Comparison between the proposed variational vortex dynamics model and Richaud *et al.* [36] model when vortices are initialized with a velocity different from the Biot-Savart induced velocity. (a) Simulation of co-rotating pair initialized with  $u_{1_0} = (-0.5i, 0.83j)$  and  $u_{2_0} = (0.5i, -0.83j)$ . (b) Co-rotating vortices initially perturbed with a radial velocity in the inward direction [36].

## VII. CONCLUSION

We introduced the use of Hamilton's principle of least action to develop a variational formulation for vortex dynamics. The developed model is fundamentally different from previous models in the literature, which are typically devised to recover a preknown set of ODEs that are first order in position. In fact, they provide a Hamiltonian formulation of the vortex motion induced by the Biot-Savart law. In contrast, the model presented here is based on formal variational principles for a continuum of inviscid fluid. As such, the model is dynamic in nature, constituted of second-order ODEs in position, which allows arbitrary initial velocities and external forces (e.g., electromagnetic). The model provided rich and intriguing dynamics for counter and co-rotating vortex pairs. In the limit to a vanishing core size, the Biot-Savart behavior is recovered. For a finite core size, there is a multi-timescale behavior: a slow dynamics that resembles the Biot-Savart motion and a fast dynamics that results in rapid oscillations around the Biot-Savart motion. However, for some given initial conditions, the averaged motion is considerably different from the Biot-Savart motion. The situation becomes interesting when an electric field is applied to a charged particle inside the vortex core. In this case, the interaction between the electrodynamic force and the hydrodynamic vortex force leads to nonintuitive behavior. For example, when a pair of counter-rotating vortices was pulled away from each other by the electric force, they moved normal to this force and opposite to their initial Biot-Savart motion; and when they were pulled in the same direction of their initial velocity, they attracted to one another (normal to the applied force). This interesting nonlinear dynamics presents the developed dynamical model as a rich example in geometric mechanics and control where concepts of anholonomy, geometric phases, and nonlinear controllability can be demonstrated. The dynamical model is also applicable to three-dimensional flows as long as the flow can be reconstructed from a few set of variables (e.g., location and strength of vortex filaments and rings), which will be tackled in future exploitation of the current variational model.

## ACKNOWLEDGMENTS

This material is based upon work supported by National Science Foundation Grant No. CBET-2005541. The first author would like to thank Dr. Mahmoud Abdelgalil at the University of California Irvine for fruitful discussions.

**APPENDIX A: FLOW KE INTEGRALS**

The two-dimensional KE is given as

$$T = \frac{\rho}{2} \int_A (\nabla\phi)^2 dA, \quad (\text{A1})$$

substituting the following relations:

$$u = \frac{\partial\psi}{\partial y}, \quad v = \frac{-\partial\psi}{\partial x}, \quad \omega_z = \frac{\partial v}{\partial x} - \frac{\partial u}{\partial y} = 0, \quad (\text{A2})$$

and the integral reads as

$$T = \frac{\rho}{2} \int_A \left( u \frac{\partial\psi}{\partial y} - v \frac{\partial\psi}{\partial x} - \psi \omega_z \right) dA = \frac{\rho}{2} \int_A \left( \frac{\partial(u\psi)}{\partial y} - \frac{\partial(v\psi)}{\partial x} \right) dA = \frac{\rho}{2} \int_A \psi \omega_z dA. \quad (\text{A3})$$

Equation (A3) applies for irrotational and rotational flows; however, we restrict the current analysis for irrotational flows only. The KE integral is computed over a multiply connected domain and, to transform the area integral to a line, one using Stokes' theorem; the domain must be transformed to a simply connected domain by the creation of fictitious barriers, as shown in Fig. 1. Then, the KE integral reads as

$$T = -\frac{\rho}{2} \oint_{R+\sigma_i+c_i} \psi \mathbf{u} \cdot d\mathbf{l} = -\frac{\rho}{2} \int_{R+\sigma_i+c_i} \psi d\phi. \quad (\text{A4})$$

The above expression is evaluated over the domain boundaries while taking into consideration the cyclic behavior of the multivalued function  $\phi$ , and assuming  $r_{ij} \gg a$ . The result is represented as

$$\begin{aligned} T &= -\frac{\rho}{2} \left[ \int_{c_i} \psi d\phi + \int_R \psi d\phi + \int_{\sigma_i} \psi d\phi \right] \\ &= -\frac{\rho}{2} \left[ \sum_{i \neq j} \sum \Gamma_i \psi_j|_i + \sum \Gamma_i \psi_i|_{c_i} + \Psi|_R \Gamma_R + \sum \Gamma_i \Psi|_R \right]. \end{aligned} \quad (\text{A5})$$

Equation (A5) concludes the KE computation and further analysis along with more simplifications are discussed in Sec. IV A 1.

**APPENDIX B:  $\partial_t \phi$  LAGRANGIAN CALCULATION**

Equation (29) is decomposed into two separate integrals,  $I_y$  and  $I_x$ ,

$$\frac{d}{dt} \left( \frac{\partial \mathcal{L}_{\phi_t}}{\partial \dot{x}_i} \right) - \frac{\partial \mathcal{L}_{\phi_t}}{\partial x_i} = \rho \dot{y}_i \left[ \underbrace{\partial_{y_i} \int \partial_{x_i} \phi_i dA}_{I_y} - \underbrace{\partial_{x_i} \int \partial_{y_i} \phi_i dA}_{I_x} \right]. \quad (\text{B1})$$

Relying on the reciprocal property of the potential function  $\phi$  between the parametrization  $(x, y)$  co-ordinates and generalized one  $(x_i, y_i)$ ,

$$\partial_{y_i} \phi_i = -\partial_y \phi_i, \quad \partial_{x_i} \phi_i = -\partial_x \phi_i, \quad (\text{B2})$$

the  $I_y$  integral can be simplified and transformed to a boundary one as

$$I_y = \partial_{y_i} \int \partial_{x_i} \phi_i dA = -\partial_{y_i} \int \partial_x \phi_i dx dy = -\partial_{y_i} \int_{\partial} \phi_i dy. \quad (\text{B3})$$

The integral is evaluated for each boundary in Fig. 1. Without loss of generality, if the barriers are taken parallel to the  $x$  axis, then  $I_y$  will be

$$I_y = -\partial_{y_i} \left\{ \sum_{\substack{j \\ i \neq j}} \int_{c_j} \phi_i dy + \int_R \phi_i dy + \int_{\sigma_i^+} \phi_i dy + \int_{\sigma_i^-} \phi_i dy + \int_{c_i} \phi_i dy \right\}. \quad (\text{B4})$$

The last and second integrals will vanish when  $\phi_i$  is treated as a single-valued function after constructing the barriers. Moreover, the third and fourth integrals will vanish, the former because of the barrier location and the latter due to selecting  $\phi_i^- = 0$ ; hence, we are left with the first integral. The differentiation can act over the first integrand because the integral boundary  $c_j$  is independent of  $y_i$  (i.e., no need for the Leibniz rule). The final form of the  $I_y$  integral is

$$I_y = -\sum_{\substack{j \\ i \neq j}} \int_{c_j} \partial_{y_i} \phi_i dy, \quad (\text{B5})$$

where it is evaluated numerically over the  $j$ th vortex boundary.

The  $I_x$  integral is computed following the same analysis, and it can be written as

$$I_x = -\partial_{x_i} \left\{ \sum_{\substack{j \\ i \neq j}} \int_{c_j} \phi_i dx + \int_R \phi_i dx + \int_{\sigma_i^+} \phi_i dx + \int_{\sigma_i^-} \phi_i dx + \int_{c_i} \phi_i dx \right\}. \quad (\text{B6})$$

Again, as before, the second, fourth, and last terms vanish with the same analogy. However, the third term will not vanish as  $\phi_i^+ = 2\pi$ , resulting in

$$I_x = -\partial_{x_i} \left\{ \sum_{\substack{j \\ i \neq j}} \int_{c_j} \phi_i dx + \Gamma_i(r_\infty - x_i - a) \right\} = -\sum_{\substack{j \\ i \neq j}} \int_{c_j} \partial_{x_i} \phi_i dx + \Gamma_i. \quad (\text{B7})$$

The end result can be substituted back in Eq. (29) to get Eq. (30).

### 1. Numerical Integration

The numerical evaluation of the terms  $I_{x_{ij}}$ ,  $I_{y_{ij}}$  is given as

$$I_{x_{ij}} = \frac{\Gamma_i}{2\pi} \left[ \int_{x_j+a}^{x_j-a} \frac{-[y_j - \sqrt{a^2 - (x-x_j)^2} - y_i]}{(x-x_i)^2 + [y_j - \sqrt{a^2 - (x-x_j)^2} - y_i]^2} dx + \int_{x_j-a}^{x_j+a} \frac{-[y_j + \sqrt{a^2 - (x-x_j)^2} - y_i]}{(x-x_i)^2 + [y_j + \sqrt{a^2 - (x-x_j)^2} - y_i]^2} dx \right], \quad (\text{B8})$$

$$I_{y_{ij}} = \frac{\Gamma_i}{2\pi} \left[ \int_{y_j+a}^{y_j-a} \frac{x_j + \sqrt{a^2 - (y-y_j)^2} - x_i}{(y-y_i)^2 + [x_j + \sqrt{a^2 - (y-y_j)^2} - x_i]^2} dy + \int_{y_j-a}^{y_j+a} \frac{x_j - \sqrt{a^2 - (y-y_j)^2} - x_i}{(y-y_i)^2 + [x_j - \sqrt{a^2 - (y-y_j)^2} - x_i]^2} dy \right]. \quad (\text{B9})$$

## APPENDIX C: COMPARISON WITH RAGAZZO'S HAMILTONIAN

A Hamiltonian formulation for the derived Lagrangian in Sec. IV is computed relying on the Legendre transformation [8]. The transformation is

$$H(\mathbf{q}, \mathbf{p}, t) = \sum_i \dot{q}_i p_i - L(\mathbf{q}, \dot{\mathbf{q}}, t), \quad (\text{C1})$$

where  $p_i$ 's are the generalized momenta given by

$$p_i = \frac{\partial L(\mathbf{q}, \dot{\mathbf{q}}, t)}{\partial \dot{q}_i}. \quad (\text{C2})$$

Recall the derived Lagrangian in Eq. (16) and substitute it into Eq. (C2); then the generalized momenta is

$$p_i = \frac{\partial L_{\phi_i}}{\partial \dot{q}_i} + \sum m_i \dot{q}_i, \quad (\text{C3})$$

where the first term is determined from Eq. (26) (whose detailed computation is given in Appendix B). The final form for the first term in Eq. (C3) includes a numerical integration over the cores circumferences, as shown in Eq. (B7). To simplify the Legendre transformation analysis and to allow for comparison with the Ragazzo *et al.* [33] Hamiltonian, massive point vortices without cores are considered instead of vortex patches. As a result, the integrals  $I_{x_{ij}}$ ,  $I_{y_{ij}}$  defined in (31) vanish. By this, and relying on Eq. (B7), Eq. (C3) yields

$$p_i = \sum m_i \dot{q}_i - \Gamma_i \rho (q_i \times \mathbf{e}_3), \quad (\text{C4})$$

and the Hamiltonian takes the form

$$\mathcal{H} = \sum \frac{1}{2m_i} \|p_i + \Gamma_i \rho (q_i \times \mathbf{e}_3)\|^2 - T. \quad (\text{C5})$$

Interestingly, the previous results are in agreement with the Hamiltonian and generalized momenta of Ragazzo *et al.* [33] (there is a sign difference because of the arbitrary sign definition for the stream function) as presented below,

$$\mathbf{p}_j = \sum m_j \dot{\mathbf{q}}_j + \frac{\Gamma_j \rho}{2} (\mathbf{q}_j \times \mathbf{e}_3), \quad (\text{C6})$$

$$\mathcal{H} = \sum \frac{1}{2m_j} \left\| \mathbf{p}_j - \frac{\Gamma_j \rho}{2} (\mathbf{q}_j \times \mathbf{e}_3) \right\|^2 + (-\rho W). \quad (\text{C7})$$

Also, setting the core size to zero in our formulation (so the integrals  $I_{x_{ij}}$ ,  $I_{y_{ij}}$  vanish) while considering nonzero core mass (i.e., considering massive point vortices), the resulting equations of motion are exactly the same as those by Ragazzo *et al.* [33].

- 
- [1] H. v. Helmholtz, *Über integrale der hydrodynamischen gleichungen, welche den wirbelbewegungen entsprechen* (Deutsch, Germany, 1858).
  - [2] H. v. Helmholtz, LXIII. On integrals of the hydrodynamical equations, which express vortex-motion, *London Edinburgh Dublin Philos. Mag. J. Sci.* **33**, 485 (1867).
  - [3] J. Clerk-Maxwell, Remarks on the mathematical classification of physical quantities, *Proc. London Math. Soc.* **s1-3**, 224 (1869).
  - [4] H. Lamb, *Hydrodynamics* (Cambridge University Press, Cambridge, UK, 1924).
  - [5] L. M. Milne-Thomson, *Theoretical Aerodynamics* (Dover Publications, New York, 1973).

- [6] P. K. Newton, *The N-vortex Problem: Analytical Techniques* (Springer Science & Business Media, New York, 2013), Vol. 145.
- [7] G. Kirchhoff and K. Hensel, *Vorlesungen über mathematische Physik* (Druck und Verlag von BG Teubner, Wiesbaden, Germany, 1883), Vol. 1.
- [8] H. Goldstein, *Classical Mechanics*, 2nd ed. (Addison-Wesley, San Francisco, 1980).
- [9] C. Lanczos, The variational principles of mechanics, in *The Variational Principles of Mechanics* (University of Toronto Press, Toronto, Canada, 2020).
- [10] C. Lin, On the motion of vortices in two dimensions: I. Existence of the Kirchhoff-Routh function, [Proc. Natl. Acad. Sci. USA \*\*27\*\*, 570 \(1941\)](#).
- [11] C. Lin, On the motion of vortices in two dimensions—II Some further investigations on the Kirchhoff-Routh function, [Proc. Natl. Acad. Sci. USA \*\*27\*\*, 575 \(1941\)](#).
- [12] G.-H. Cottet, P. D. Koumoutsakos *et al.*, *Vortex Methods: Theory and Practice* (Cambridge University Press, Cambridge, UK, 2000), Vol. 8.
- [13] S. V. Alekseenko, P. A. Kuibin, and V. L. Okulov, *Theory of Concentrated Vortices: An Introduction* (Springer Science & Business Media, New York, 2007).
- [14] H. Aref, Point vortex dynamics: A classical mathematics playground, [J. Math. Phys. \*\*48\*\*, 065401 \(2007\)](#).
- [15] R. L. Seliger and G. B. Whitham, Variational principles in continuum mechanics, [Proc. R. Soc. London A \*\*305\*\*, 1 \(1968\)](#).
- [16] A. A. Tchieu and A. Leonard, A discrete-vortex model for the arbitrary motion of a thin airfoil with fluidic control, [J. Fluids Struct. \*\*27\*\*, 680 \(2011\)](#).
- [17] H. E. Taha and A. S. Rezaei, On the high-frequency response of unsteady lift and circulation: A dynamical systems perspective, [J. Fluids Struct. \*\*93\*\*, 102868 \(2020\)](#).
- [18] S. M. Ramodanov, Motion of a circular cylinder and a vortex in an ideal fluid, [Regul. Chaot. Dyn. \*\*6\*\*, 33 \(2001\)](#).
- [19] A. V. Borisov and I. S. Mamaev, Integrability of the problem of the motion of a cylinder and a vortex in an ideal fluid, [Math. Notes \*\*75\*\*, 19 \(2004\)](#).
- [20] A. V. Borisov, I. S. Mamaev, and S. M. Ramodanov, Motion of a circular cylinder and n point vortices in a perfect fluid, [arXiv:nlin/0502029](#).
- [21] A. V. Borisov, I. S. Mamaev, and S. M. Ramodanov, Dynamics of a circular cylinder interacting with point vortices, *Discrete Contin. Dyn. Syst. Ser. B* **5**, 35 (2005).
- [22] A. V. Borisov, I. S. Mamaev, and S. M. Ramodanov, Dynamic interaction of point vortices and a two-dimensional cylinder, [J. Math. Phys. \*\*48\*\*, 065403 \(2007\)](#).
- [23] S. M. Ramodanov and S. V. Sokolov, Dynamics of a circular cylinder and two point vortices in a perfect fluid, [Regul. Chaot. Dyn. \*\*26\*\*, 675 \(2021\)](#).
- [24] B. N. Shashikanth, J. E. Marsden, J. W. Burdick, and S. D. Kelly, The Hamiltonian structure of a two-dimensional rigid circular cylinder interacting dynamically with  $N$  point vortices, [Phys. Fluids \*\*14\*\*, 1214 \(2002\)](#).
- [25] J. D. Eldredge, *Mathematical Modeling of Unsteady Inviscid Flows* (Springer, New York, 2019).
- [26] C. Wang and J. D. Eldredge, Low-order phenomenological modeling of leading-edge vortex formation, [Theor. Comput. Fluid Dyn. \*\*27\*\*, 577 \(2013\)](#).
- [27] S. Michelin and S. G. Llewellyn Smith, An unsteady point vortex method for coupled fluid–solid problems, [Theor. Comput. Fluid Dyn. \*\*23\*\*, 127 \(2009\)](#).
- [28] P. Tallapragada and S. D. Kelly, Reduced-order modeling of propulsive vortex shedding from a free pitching hydrofoil with an internal rotor, in *Proceedings of the 2013 American Control Conference* (IEEE, New York, NY, 2013), pp. 615–620.
- [29] A. A. Hussein, H. E. Taha, S. Ragab, and M. R. Hajj, A variational approach for the dynamics of unsteady point vortices, [Aerosp. Sci. Technol. \*\*78\*\*, 559 \(2018\)](#).
- [30] C. Brown, Jr. and W. Michael, Effect of leading-edge separation on the lift of a delta wing, [J. Aeronaut. Sci. \*\*21\*\*, 690 \(1954\)](#).
- [31] R. Salmon, Hamiltonian fluid mechanics, [Annu. Rev. Fluid Mech. \*\*20\*\*, 225 \(1988\)](#).
- [32] D. M. Chapman, Ideal vortex motion in two dimensions: Symmetries and conservation laws, [J. Math. Phys. \*\*19\*\*, 1988 \(1978\)](#).

- [33] C. G. Ragazzo, J. Koiller, and W. Oliva, On the motion of two-dimensional vortices with mass, *J. Nonlinear Sci.* **4**, 375 (1994).
- [34] W. Olva, The motion of two dimensional vortices with mass as a singular perturbation Hamiltonian problem, *New Trends Hamilton. Syst. Celestial Mech.* **8**, 301 (1996).
- [35] A. Richaud, V. Penna, R. Mayol, and M. Guilleumas, Vortices with massive cores in a binary mixture of Bose-Einstein condensates, *Phys. Rev. A* **101**, 013630 (2020).
- [36] A. Richaud, V. Penna, and A. L. Fetter, Dynamics of massive point vortices in a binary mixture of Bose-Einstein condensates, *Phys. Rev. A* **103**, 023311 (2021).
- [37] A. Richaud, P. Massignan, V. Penna, and A. L. Fetter, Dynamics of a massive superfluid vortex in R K confining potentials, *Phys. Rev. A* **106**, 063307 (2022).
- [38] V. V. Meleshko and H. Aref, A bibliography of vortex dynamics 1858–1956, *Adv. Appl. Mech.* **41**, 197 (2007).
- [39] S. G. L. Smith, How do singularities move in potential flow? *Physica D* **240**, 1644 (2011).
- [40] P. K. Newton, Point vortex dynamics in the post-Aref era, *Fluid Dyn. Res.* **46**, 031401 (2014).
- [41] G. Batchelor, *An Introduction to Fluid Dynamics* (Cambridge University Press, Cambridge, UK, 1967).
- [42] P. G. Saffman, *Vortex Dynamics* (Cambridge University Press, Cambridge, UK, 1992).
- [43] L. M. Milne-Thomson, *Theoretical Hydrodynamics* (Dover Publications, New York, 1996).
- [44] J.-Z. Wu, H.-Y. Ma, and M.-D. Zhou, *Vorticity and Vortex Dynamics* (Springer Science & Business Media, New York, 2007).
- [45] C. Truesdell, *The Kinematics of Vorticity* (Indiana University Press, Bloomington, IN, 1954).
- [46] H. Bateman, Notes on a differential equation which occurs in the two-dimensional motion of a compressible fluid and the associated variational problems, *Proc. R. Soc. London A* **125**, 598 (1929).
- [47] J. Herivel, The derivation of the equations of motion of an ideal fluid by Hamilton’s principle, in *Mathematical Proceedings of the Cambridge Philosophical Society* (Cambridge University Press, Cambridge, UK, 1955), Vol. 51, pp. 344–349.
- [48] F. P. Bretherton, A note on Hamilton’s principle for perfect fluids, *J. Fluid Mech.* **44**, 19 (1970).
- [49] P. Penfield, Jr., Hamilton’s principle for fluids, *Phys. Fluids* **9**, 1184 (1966).
- [50] R. Hargreaves, XXXVII. A pressure-integral as kinetic potential, *London Edinburgh Dublin Philos. Mag. J. Sci.* **16**, 436 (1908).
- [51] J. Serrin, Mathematical principles of classical fluid mechanics, in *Fluid Dynamics I/Strömungsmechanik I* (Springer, Berlin, Heidelberg, 1959), pp. 125–263.
- [52] J. C. Luke, A variational principle for a fluid with a free surface, *J. Fluid Mech.* **27**, 395 (1967).
- [53] M. I. Loffredo, Eulerian variational principle for ideal hydrodynamics and two-fluid representation, *Phys. Lett. A* **135**, 294 (1989).
- [54] P. J. Morrison, Hamiltonian description of the ideal fluid, *Rev. Mod. Phys.* **70**, 467 (1998).
- [55] V. L. Berdichevsky, Continuum mechanics, in *Variational Principles of Continuum Mechanics: I. Fundamentals* (Springer, Berlin, Heidelberg, 2009), pp. 67–115.
- [56] K. Yasue, A variational principle for the Navier-Stokes equation, *J. Funct. Anal.* **51**, 133 (1983).
- [57] R. R. Kerswell, Variational principle for the Navier-Stokes equations, *Phys. Rev. E* **59**, 5482 (1999).
- [58] D. A. Gomes, A variational formulation for the Navier-Stokes equation, *Commun. Math. Phys.* **257**, 227 (2005).
- [59] G. L. Eyink, Stochastic least-action principle for the incompressible Navier-Stokes equation, *Physica D* **239**, 1236 (2010).
- [60] H. Fukagawa and Y. Fujitani, A variational principle for dissipative fluid dynamics, *Prog. Theor. Phys.* **127**, 921 (2012).
- [61] C. R. Galley, D. Tsang, and L. C. Stein, The principle of stationary nonconservative action for classical mechanics and field theories, [arXiv:1412.3082](https://arxiv.org/abs/1412.3082).
- [62] F. Gay-Balmaz and H. Yoshimura, A Lagrangian variational formulation for nonequilibrium thermodynamics. Part II: Continuum systems, *J. Geom. Phys.* **111**, 194 (2017).
- [63] J. A. Burns, *Introduction to the Calculus of Variations and Control with Modern Applications* (CRC Press, Boca Raton, FL, 2013).

- [64] N. J. Zabusky, M. Hughes, and K. Roberts, Contour dynamics for the Euler equations in two dimensions, *J. Comput. Phys.* **30**, 96 (1979).
- [65] D. Pullin, Contour dynamics methods, *Annu. Rev. Fluid Mech.* **24**, 89 (1992).
- [66] M. Melander, N. Zabusky, and A. Styczek, A moment model for vortex interactions of the two-dimensional Euler equations. Part 1. Computational validation of a Hamiltonian elliptical representation, *J. Fluid Mech.* **167**, 95 (1986).
- [67] G. S. Deem and N. J. Zabusky, Vortex waves: Stationary “v states,” interactions, recurrence, and breaking, *Phys. Rev. Lett.* **40**, 859 (1978).
- [68] R. Pierrehumbert, A family of steady, translating vortex pairs with distributed vorticity, *J. Fluid Mech.* **99**, 129 (1980).
- [69] P. Saffman and R. Szeto, Equilibrium shapes of a pair of equal uniform vortices, *Phys. Fluids* **23**, 2339 (1980).
- [70] A. H. Nayfeh and D. T. Mook, *Nonlinear Oscillations* (Wiley, New York, 2008).
- [71] A. H. Nayfeh, *Introduction to Perturbation Techniques* (Wiley, New York, 2011).
- [72] F. Bullo and A. D. Lewis, *Geometric Control of Mechanical Systems: Modeling, Analysis, and Design for Simple Mechanical Control Systems* (Springer, New York, 2019), Vol. 49.
- [73] A. M. Hassan and H. E. Taha, Differential-geometric-control formulation of flapping flight multi-body dynamics, *J. Nonlinear Sci.* **29**, 1379 (2019).
- [74] H. E. Taha, L. P. Olea, N. Khalifa, C. Gonzalez, and A. S. Rezaei, Geometric-control formulation and averaging analysis of the unsteady aerodynamics of a wing with oscillatory controls, *J. Fluid Mech.* **928**, A30 (2021).
- [75] W. S. Levine, Open-loop control using oscillatory inputs, in *The Control Systems Handbook* (CRC Press, Boca Raton, 2018), pp. 1191–1211.
- [76] J. E. Marsden, O. M. O’Reilly, F. J. Wicklin, and B. W. Zombros, Symmetry, stability, geometric phases, and mechanical integrators, *Nonlinear Sci. Today* **1**, 4 (1991).
- [77] J. E. Marsden, Geometric foundations of motion and control, in *Motion, Control, and Geometry: Proceedings of a Symposium, Board on Mathematical Science, National Research Council Education* (National Academies Press, Washington, DC, 1997).
- [78] A. M. Hassan and H. E. Taha, Geometric control formulation and nonlinear controllability of airplane flight dynamics, *Nonlinear Dyn.* **88**, 2651 (2017).
- [79] H. E. Taha, A. Hassan, and M. Fouda, Nonlinear flight physics of the lie bracket roll mechanism, *Nonlinear Dyn.* **106**, 1627 (2021).